JCTC Journal of Chemical Theory and Computation

Article

pubs.acs.org/JCTC

Partial Atomic Charges and Screened Charge Models of the Electrostatic Potential

Bo Wang and Donald G. Truhlar*

Department of Chemistry and Supercomputing Institute, University of Minnesota, 207 Pleasant Street S.E., Minneapolis, Minnesota 55455-0431, United States

Supporting Information

ABSTRACT: We propose a new screened charge method for calculating partial atomic charges in molecules by electrostatic potential (ESP) fitting. The model, called full density screening (FDS), is used to approximate the screening effect of full charge densities of atoms in molecules. The results are compared to the conventional ESP fitting method based on point charges and to our previously proposed outer density screening (ODS) method, in which the parameters are reoptimized for the present purpose. In ODS, the charge density of an atom is represented by the sum of a point charge and a smeared negative charge distributed in a Slater-type orbital (STO). In FDS, the charge density of an atom is taken to be the sum of the charge density of the neutral atom and a partial atomic charge (of either sign) distributed in an STO. The ζ values of the STOs used in these two models are optimized in the present study to best reproduce the electrostatic potentials. The quality of the fit to the electrostatics is improved in the screened charge methods, especially for the regions that are within one van der Waals radius of the centers of atoms. It is also found that the charges derived by fitting electrostatic potentials with screened charges are less sensitive to the positions of the fitting points than are those derived with conventional electrostatic fitting. Moreover, we found that the electrostatic-potential-fitted (ESP) charges from the screened charge methods are similar to those from the point-charge method except for molecules containing the methyl group, where we have explored the use of restraints on nonpolar H atoms. We recommend the FDS model if the only goal is ESP fitting to obtain partial atomic charges or a fit to the ESP field. However, the ODS model is more accurate for electronic embedding in combined quantum mechanical and molecular mechanical (QM/MM) modeling and is more accurate than point-charge models for ESP fitting, and it is recommended for applications involving QM/MM methods. Since the screened charges describe the electrostatic potentials more accurately than point charges, since they asymptotically act as point charges at long distances, and since the electrostatic potential in terms of the screened charges is still a sum of functions centered at the atoms, the screened-charge representation of the electrostatic potential can be used in the same way as the conventional point-charge representation to model the electrostatic interactions, but it is more realistic. For the H atom and p block elements, the error in the fit to the electrostatic potential is reduced by about a factor of 3, and the sensitivity of the derived partial atomic charges to the choice of fitting points is reduced by about a factor of 2. For s and d block elements, there are also improvements in the inner regions but not necessarily in the outer regions.

1. INTRODUCTION

Partial atomic charges play an important role in molecular simulations. They constitute a very convenient way to describe the charge distribution within a molecule, and they can be used to compute the noncovalent electrostatic interactions within or among molecules in molecular mechanics. Moreover, the partial atomic charges are useful as an analysis tool that reflects changes in an atom's local chemical environment and bonding.

Partial atomic charge is not a quantum mechanical observable, and it is ambiguous to assign a certain portion of the electron density to each atom in a molecule. As a consequence, various charge models have been proposed to determine the partial atomic charges. They can be classified into four categories.[1] Class I charges are based on concepts and formulas originating in classical mechanical models, such as classical electronegativity equalization.[2] Class II charges are based on partitioning of the wave function or the electron density from quantum mechanical calculations; examples include Mulliken population analysis,[3] Löwdin population analysis,[4] and Hirshfeld population analysis.[5−7] Such partitions are intrinsically ambiguous. Class III charges are computed by constraining the charges to reproduce, usually in a least-squares sense, calculated physical observables, such as the electrostatic potentials.[8−16] Class IV charges are derived by semiempirical mapping of the partial atomic charges from other charge models (generally of class II) to reproduce experimental observables.[1,17−19]

Electrostatic-potential-fitted (ESP fitted) charges, which are fitted to reproduce quantum mechanically calculated electrostatic potentials, belong to class III. The method was first developed by Momany,[8] followed by Cox and Williams,[9] Singh and Kollman,[10] Chirlian and Francl,[11] Breneman and Wiberg,[12] and others. The most significant difference among various schemes is the selection of fitting points. The ESP charges can reproduce the electrostatic potentials far from the molecule quite well and near the molecule reasonably well, and they are widely used to treat the noncovalent intramolecular and intermolecular electrostatic interactions in molecular modeling. They also lead to reasonably accurate values for some physical

Received: December 23, 2011
Published: March 30, 2012

observables, such as the dipole moment. Moreover, compared with class II charges, ESP charges for many molecules show smaller variations with the quantum mechanical level of theory and the basis set, and they converge to definite values with increasing basis-set size, whereas population analysis charges can and often do become unphysical for large basis sets.

Conventional ESP charges face some challenges. First, the point-charge approximation breaks down when the fitted points are close to the centers of atoms, for example, when they are closer than about one van der Waals radius. Therefore, we cannot fit the points that are too close to the centers of the atoms in the fitting process, and the resulting fitting points are far from buried atoms, that is, from the atoms that are not near the molecular surface. As a consequence, the charges of buried atoms are poorly determined. Mathematically, this shows up as ill-conditioning in the linear equations of the least-squares ESP fitting process.[20] Second, the fitted charges are not numerically stable with respect to the molecular geometries. For example, unphysical conformational dependence has been found in electrostatic fitting.[10,12] This causes problems in the calculations of intramolecular interactions. One of the most widely used approaches to circumvent these problems is the restrained ESP (RESP) method, in which a penalty function is added for certain atoms in the fitting procedure to restrain their charges from deviating widely from target values. The target charges can be zero,[13] Hirshfeld charges,[14] or Bader charges.[16] However, RESP charges can also suffer some stability problems.[15]

One of the intrinsic problems of conventional ESP fitted charges is that only point charges at the nuclei are employed, and this does not include the charge penetration effect. That is why only points outside the electron distribution of the molecules can be used for meaningful fitting. However, the charge penetration effect can be quite significant even outside the van der Waals surface, and various procedures have been proposed to include this effect in molecular modeling.[21−31] Including the charge penetration effect can greatly improve the description of the electrostatics for points within or close to the van der Waals surfaces of the molecules.

In the present study, we seek to derive ESP charges by using new screened charge models that include the charge penetration effect. Our new models are based on modified versions of the screened charge model proposed in a previous study.[29] The electron densities around atoms are delocalized, and the atoms in the molecules are approximated as spherically symmetric delocalized charge distributions. In section 2, we will introduce the screened charge models to include the charge penetration effect and describe the procedure to derive the ESP charges. Section 3 will give the computational details. Section 4 will present the results and a detailed analysis of the new methods. Section 5 will summarize the main conclusions.

2. METHODS

2.1. Two Kinds of Screened Charge Models. We improve the point-charge model by considering the detailed electronic structure of the atoms. We make the approximation that the electrons in the atoms of the molecule, complex, or cluster under consideration are distributed as a sum of spherical distributions centered at the nuclei. Two kinds of screened models are proposed; we will call them outer-density screening (ODS) and full-density screening (FDS).

The ODS method was presented previously,[29] but it is reparametrized in the present work. In this model, we distribute a part of electron density in a Slater-type orbital (STO). At a distance r from its nucleus, the effective charge of atom A is written as[29]

$$q_{A,\mathrm{eff}} = q_A + n_{\mathrm{screen}} f_{Z_A}(\zeta_{Z_A} r) \exp(-2\zeta_{Z_A} r) \quad (1)$$

where q_A is the partial atomic charge of atom A, ζ_{Z_A} is a parameter depending on the atomic number Z_A of atom A, n_{screen} is the number of electrons included in the STO, and f_{Z_A} is a polynomial factor derived in the previous paper.[29] The parameter n_{screen} equals $1 - q$ for H atoms and 1 for other atoms.[29] The present model differs from the model proposed in the previous work in two aspects of the parametrization. First, metal atoms are screened in the present study, while they are not screened in the previous study. Second, ζ_{Z_A} values are recommended for all elements in the present study (see sections 2.4 and 2.5).

One of the drawbacks of the ODS model is that only part of the penetration effect is included since only n_{screen} electrons are in the screening distribution. Therefore, in the second model, which is called the full-density screening (FDS) model, we approximate the charge density of an atom in a molecule, except for H atoms, as the sum of the charge density of the neutral atom and a charge distribution (which is positive for positive partial atomic charge and negative for negative partial atomic charge) in an STO. The analytical expressions for the effective charges of neutral atoms are taken from Strand and Bonham's work.[32] For a H atom, we assume that the atom is composed of a nucleus and an electron density distributed in the hydrogen 1s orbital, which is a special case of an STO.

The effective charge of a neutral atom A in the work of Strand and Bonham is expressed as

$$Z_{\mathrm{eff,A}}(r) = Z_A\left(\sum_i {}^{a}\gamma_i \exp(-{}^{a}\lambda_i r) + r\sum_j {}^{b}\gamma_i \exp(-{}^{b}\lambda_j r)\right) \quad (2)$$

where r is the distance from the nucleus, $Z_{\mathrm{eff,A}}(r)$ is the effective charge of the neutral atom, Z_A is the atomic number, and γ_i and λ_i are fitted parameters. The partial atomic charge q_A, which can be either positive (a hole distribution) or negative (a particle distribution), is distributed in an STO:

$$\varphi_{(n)} = Dr^{n-1} \exp(-\zeta_{Z_A} r) \quad (3)$$

where n is the period number of the element and D is the factor that normalizes the orbital to unity. Thus, the effective charge due to the STO is

$$q_{A,\mathrm{STO}} = q_A - q_A f_{Z_A}(\zeta_{Z_A} r) \exp(-2\zeta_{Z_A} r) \quad (4)$$

where f_{Z_A} is the same polynomial factor as already introduced in eq 1.

Therefore, the total effective charge for all atoms except H atoms is obtained by adding eqs 2 and 4 to get

$$q_{A,\mathrm{eff}} = Z_{\mathrm{eff,A}}(r) + q_A - q_A f_{Z_A}(\zeta_{Z_A} r) \exp(-2\zeta_{Z_A} r) \quad (5)$$

For H atoms, the total effective charge can be derived from eq 1 by substituting $1 - q_A$ for n_{screen}:

$$q_{H,\mathrm{eff}} = q_H + (1 - q_H) f_H(\zeta_H r) \exp(-2\zeta_H r) \quad (6)$$

Values of the exponents ζ_{Z_A} of the STOs will be recommended for all elements in sections 2.4 and 2.5.

2.2. ESP Charges. To derive the ESP charges from quantum mechanical (QM) electrostatic potentials, we define the error function to be minimized during the fitting process as

$$y(q_1, q_2, ...q_N) = \sum_{k=1}^{m} [V_k^{QM} - V_k^{ESP}(q_1, q_2, ...q_N)]^2 \quad (7)$$

where m is the total number of fitting points, N is the number of atoms in the molecule, V_k^{QM} is the QM electrostatic potential, q_i is the fitted partial atomic charge (i = 1, 2, ...N), and $V_k^{ESP}(q_1, q_2, ...q_N)$ is the fitted electrostatic potential calculated from the point charges or the screened charges. The fitted electrostatic potential is expressed as

$$\begin{aligned} V_k^{ESP}(q_1, q_2, ...q_N) &= \sum_{i=1}^{N} q_i/r_{ik} && \text{(point charge model)} \\ &= \sum_{i=1}^{N} \frac{q_i + n_{screen} f(\zeta_i r_{ik}) \exp(-2\zeta_i r_{ik})}{r_{ik}} && \text{(ODS)} \\ &= \sum_{i=1,\text{not H atom}}^{N-N_H} \frac{Z_{eff,i}(r_{ik}) + q_i - q_i f(\zeta_i r_{ik}) \exp(-2\zeta_i r_{ik})}{r_{ik}} && \text{(FDS)} \\ &\quad + \sum_{i=1,\text{H atom}}^{N_H} \frac{q_i + (1 - q_i) f(\zeta_i r_{ik}) \exp(-2\zeta_i r_{ik})}{r_{ik}} \end{aligned} \quad (8)$$

where N_H is the number of H atoms, r_{ik} is the distance between atom i and fitting point k, and ζ_i is the exponential parameter of the STO for atom i.

Finding the minimum of y subject to the conservation of charge is equivalent to finding the stationary points of the Lagrangian function z:

$$z = y(q_1, q_2, ...q_N) + \lambda(\sum_{i=1}^{N} q_i - q_{tot}) \quad (9)$$

where q_{tot} is the total charge of the molecule. We solve the n + 1 linear equations obtained by $\partial z/\partial q_i = 0$ and $\partial z/\partial \lambda = 0$ to get the partial atomic charges.

2.3. Selection of Fitting Points. Another choice we need to make is which points to use for fitting the electrostatic potentials. We have tested 66 point selection schemes, and we will present results for six of them. The first two are the MK[10] and ChElPG[12] point selection schemes. They are well-defined in the literature, and since a detailed description can be found in refs 10 and 12, we only summarize them briefly here. In the MK scheme, the fitting points are selected using the Connolly surface algorithm from four shells of 1.4, 1.6, 1.8, and 2.0 times the van der Waals radius.[10] In the ChElPG scheme, the fitting points are selected from a Cartesian grid around the molecule with nodes spaced 0.3 Å apart, including 2.8 Å of headspace on all sides and excluding the points that fall inside the van der Waals radius of any atom.[12] We will also briefly consider the earlier ChElP[11] scheme.

The other schemes tested here are formulated in various ways, and the four new schemes for which results are presented are based on selecting points from a Cartesian grid with nodes spaced by 0.2 Å. Different fitting points are selected from the grid of points in different schemes. In particular, we selected the fitting points k that satisfy:

$$\min_j\{r_{jk} - aR_j\} > 0$$
$$\min_j\{r_{jk} - bR_j\} < 0 \quad (10)$$

where j = 1, 2, ..., N, a and b are parameters that specify the scheme, r_{jk} is the distance between fitting point k and atom j, and R_j is the van der Waals radius of atom j, which is from the consistent van der Waals radii suggested in the *CRC Handbook of Chemistry and Physics*.[33] The distinguishing parameters of the four new schemes for which we present results are given in Table 1. For example, in scheme C, the fitting points are in a shell with inner radius 1.4 R_i and outer radius 1.6 R_i around each atom i, but all points within 1.4 R_j of any other atom j are excluded; schemes are illustrated in Figure 1.

Table 1. Four New Schemes in the Present Study

	parameters	
scheme	A	b
A	0.6	0.8
B	1.0	1.2
C	1.4	1.6
D	1.8	2.0

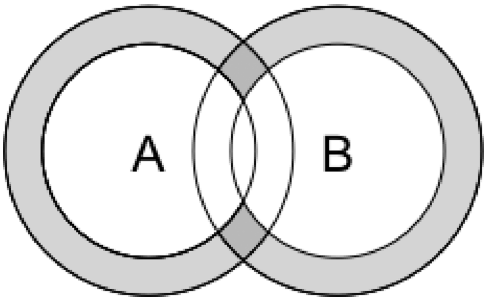

Figure 1. For schemes A–D of Table 1, points in the shaded area, where the inner sphere around each atom j has radius aR_j and the outer sphere has radius bR_j. This shaded area also serves to illustrate the testing layers of eq 11. Layer L has inner sphere radius LR_j and outer sphere radius $(L + 0.1)R_j$.

2.4. Optimization of the Point Selection Scheme and the ζ Values of STOs for Common Elements. We optimize the ζ values for common elements such that the derived ESP charges can best reproduce the quantum mechanical electrostatic potentials. We started the optimization of the ζ values from the modified Strand and Bonham's parameters listed in Table 2, which are ζ = 1.32 for the H atom and half of the

dx.doi.org/10.1021/ct2009285 | J. Chem. Theory Comput. 2012, 8, 1989–1998

Table 2. Modified Strand Bonham Parameters (in a_0^{-1})[a]

atom	H	C	N	O	F
ζ	1.32	0.87	1.01	1.12	1.24
atom	Al	Si	P	S	Cl
ζ	0.68	0.74	0.81	0.88	0.95

[a]The optimized exponent for the H atom in ref 29 and half of the exponents for the outermost orbitals of ref 32 for non-H atoms.

exponents for the outermost terms in ref 32 for non-H atoms.[29,32] We multiplied the ζ parameters for all non-H atoms by a scaling factor S. Rather than optimizing the ζ value for each individual element, we optimize a common scaling factor for the best fit in the ODS and FDS models, respectively. The criterion for the best fit is explained next.

Because different point selection schemes use different fitting points, the value of the error function defined in eq 7 cannot be directly used as a criterion to compare the fitting performance among different point selection schemes. For testing, we used a Cartesian grid with nodes spaced by 0.3 Å. The testing points are grouped into layers around the molecule. Layer L includes all the points k that satisfy

$$\min_j\{r_{jk} - LR_j\} > 0$$
$$\min_j\{r_{jk} - (L + 0.1)R_j\} < 0 \quad (11)$$

for j = 1, 2, ..., N. A sample layer is illustrated in Figure 1.

Then, we define the relative root-mean-square error of electrostatic potentials in layer L in molecule j as

$$\varepsilon_{L,j} = \sqrt{\sum_{k=1}^{t}[V_k^{QM} - V_k^{ESP}(q_1, q_2, ...q_N)]^2 / \sum_{k=1}^{t} V_k^{QM^2}} \quad (12)$$

where t is the number of testing points in layer L. Then, we define the following averages of these errors. The average relative error over all 19 layers (L = 0.1, 0.2, ...1.9) for molecule j is defined as

$$\varepsilon_{all,j} = \frac{1}{19}\sum_{L=0.1}^{1.9}\varepsilon_{L,j} \quad (13)$$

and the average relative error over the outer 10 layers (those beyond the van der Waals radius) for molecule j is defined as

$$\varepsilon_{outer,j} = \frac{1}{10}\sum_{L=1.0}^{1.9}\varepsilon_{L,j} \quad (14)$$

and the average relative errors over all molecules are

$$\varepsilon_{all} = \frac{1}{M}\sum_{j=1}^{M}\varepsilon_{all,j} \quad (15)$$

$$\varepsilon_{outer} = \frac{1}{M}\sum_{j=1}^{M}\varepsilon_{outer,j} \quad (16)$$

where M is the number of molecules considered (15 in the present study); ε_{all} and ε_{outer} show the performance of the fitting.

We tested 66 point selection schemes and various scaling factors, and the point selection schemes and optimized scaling factors (S) that give the smallest ε_{outer} using the ODS and FDS models are shown in the last six rows of Table 3.

Table 3. ε_{all} and ε_{outer} and the Mean Unsigned Error (MUE) of Dipole Moments (debyes) over 15 Molecules Using the Point-Charge Model and the ODS and FDS Models

charge model	point selection scheme	S	ε_{all}	ε_{outer}	MUE of dipole moment
PC[a]	MK		0.62	0.32	0.05
PC	ChElPG		0.61	0.32	0.07
ODS	scheme C	1.4	0.42	0.27	0.06
FDS	scheme C	1.6	0.21	0.27	0.06
ODS	MK	1.4	0.42	0.27	0.06
ODS	ChElPG[b]	1.4	0.41	0.27	0.07
FDS[b]	MK[b]	1.6	0.21	0.27	0.05
FDS	ChElPG	1.6	0.21	0.27	0.06

[a]Point-charge method. [b]These are the finally recommended methods.

2.5. ζ Values for Other Elements. The ζ values have units of a_0^{-1}, and they can be converted to effective radii in Ångstroms by

$$R_{eff,Z} = C/\zeta_Z \quad (17)$$

where C = 0.5292 Å/a_0 and Z is the atomic number.

For the 10 elements in Table 2, we computed the average value of $R_{vdW,Z}/R_{eff,Z}$, where $R_{vdW,Z}$ is the van der Waals radius (in Å); in the *CRC Handbook of Chemistry and Physics*,[33] we find that $\langle R_{vdW,Z}/R_{eff,Z}\rangle = 2.93 \pm 0.30$, where the stated error is a standard deviation. Therefore, for other elements, we recommend that ζ_Z be set to 1.4 (the optimized scaling factor of the ODS method from Table 3) × 2.93 $R_{vdW,Z}^{-1}$ (= 4.10 $R_{vdW,Z}^{-1}$) for the ODS method and that ζ_Z be set to 1.6 (the optimized scaling factor of the FDS method from Table 3) × 2.93 $R_{vdW,Z}^{-1}$ (= 4.69 $R_{vdW,Z}^{-1}$) for the FDS method. Since $R_{vdW,Z}$ is available for the whole periodic table, this defines ζ_Z for all elements.

3. COMPUTATIONAL DETAILS

The electrostatic potentials at all of the fitting points and the testing points are calculated using *Gaussian 09*,[34] and these potentials are used as input for electrostatic fitting with the screened charge models in a small code that solves the linear equations arising from eq 9. We have also modified link l602 of *Gaussian 09* to make the output used by the fitting process more convenient.

For the molecules in the test suite, we used M06-2X[35,36]/6-31G*[37−39] optimized geometries with M06-2X/MG3S[40] single-point calculations. The test suite has 15 molecules, in particular $(CH_3)_2CO$, $(CH_3)_2SO$, CH_3CN, CH_3OH, H_2O, $HCONH_2$, NH_3, ClF, H_2S, $H_3SiOHAlH_3$, $H_3SiOSiH_3$, HCl, HF, PH_2CHCH_2, and PH_3.

4. RESULTS AND DISCUSSION

Three choices are required to define an ESP fitting method: (1) the charge model, which can be the point-charge (PC) method, the ODS method, or the FDS method; (2) the point selection scheme, which can be MK, ChElP, ChElPG, or any of the 63 new schemes (for example, schemes A−D of Table 1); and (3) the ζ values, which are determined by the scaling factor S for all non-H atoms. Therefore, we will use *X-Y-S* to specify a screened charge method, or *X-Y* for a point-charge method where no scaling factor is needed, where *X* represents the charge model, *Y* represents the point selection scheme, and *S* represents the scaling factor.

4.1. Overall Fitting Performance. Table 3 shows ε_{all}, ε_{outer}, and the mean unsigned errors (MUE) of their dipole moments for the point-charge model and two screened charge models. (The "error" in the dipole moment is defined as the difference between the dipole moment calculated from the electron density (as usual) and that calculated from the fitted charges.)

The first two rows of Table 3 show the results obtained by using the PC model with the MK and ChElPG point selection schemes. These are well-established and popular methods and are presented for comparison with the new methods.

The next two rows show the optimized point selection schemes and their optimized scaling factors that minimize ε_{outer} for the ODS and FDS models, respectively. The optimum ODS scheme for ε_{outer} is ODS-C-1.4, and the optimum FDS scheme for ε_{outer} is FDS-C-1.6. However, several other methods also give small ε_{outer}. The next four rows show the results with the MK and ChElPG point selection schemes using the ODS and FDS models, respectively. When we consider all of these error criteria (ε_{all}, ε_{outer}, and MUE in dipole moments), the best scheme is FDS-MK-1.6. As compared to the point-charge method, the FDS method has about the same MUE (0.05 D) in dipole moments. However, the error in the electrostatic potential averaged over the 10 outer layers is reduced by a factor of 1.2 (0.27 vs 0.32), and *the error in the electrostatic potential averaged over all 19 layers is reduced by a factor of 3* (0.21 vs 0.62). The reason for this dramatic improvement is that the point-charge model becomes very unrealistic in regions close to a nucleus. Since the FDS model includes penetration effects all the way into the nucleus, it is more realistic than the ODS model in the inner regions.

Another key conclusion from Table 3 is that conventional point selection schemes originally developed for point-charge fitting, in particular, MK and ChElPG, can also be used for electrostatic potential fitting in the screened charge models. Therefore, conventional electrostatic fitting subroutines can be improved by simply replacing the point-charge model by the screened charge models. As these point selection schemes have been implemented in popular software, such as *Gaussian 09*,[34] minimum modifications are needed to use the screened charge methods. Our final recommendation is to use the FDS-MK-1.6 method to derive ESP charges.

4.2. Stability of the Fitted Charges. The sensitivity of the fitted charges to the positions of the fitting points is one of the most important criteria for comparing the quality of the point-charge model to that of the screened charge models. Since the charge penetration effect is included in the screened charge models, fitting electrostatic potentials to screened charges is more physical than using point charges, and therefore, the fitted charges can be more stable. As the MK, ChElP, and ChElPG point selection schemes use different points for fitting, we calculated the averaged standard deviations ($\bar{\sigma}$) of charges obtained by using these three point selection schemes, and we use these values as an indication for the sensitivity. The sensitivity $\bar{\sigma}$ for molecule i is defined as

$$\bar{\sigma}_i = \frac{1}{N_i}\sum_{j=1}^{N_i}\{\frac{1}{2}[(q_{i,j,\mathrm{MK}} - \bar{q}_{i,j})^2 + (q_{i,j,\mathrm{ChElP}} - \bar{q}_{i,j})^2 + (q_{i,j,\mathrm{ChElPG}} - \bar{q}_{i,j})^2]\}^{1/2} \quad (18)$$

where

$$\bar{q}_{i,j} = \frac{1}{3}(q_{i,j,\mathrm{MK}} + q_{i,j,\mathrm{ChElP}} + q_{i,j,\mathrm{ChElPG}}) \quad (19)$$

where N_i is the number of atoms in molecule i; $q_{i,j,\mathrm{MK}}$, $q_{i,j,\mathrm{ChElP}}$, and $q_{i,j,\mathrm{ChElPG}}$ are the MK, ChElP, and ChElPG partial atomic charges (q_A) of atom j in molecule i, respectively; and $\bar{q}_{i,j}$ is the averaged MK, ChElP, and ChElPG partial atomic charge of atom j in molecule i.

The $\bar{\sigma}_i$ values for all molecules in the test suite are shown in Table 4. When $\bar{\sigma}_i$ is further averaged over 15 molecules, the value of 0.044 in the point-charge model is reduced to 0.024 in the ODS model and to 0.021 in the FDS model. This shows that *the charges obtained by fitting with the screened charge models are about a factor of 2 less sensitive to the positions of the fitting points than those obtained by the point-charge model.* This finding can also explain why the MK and ChElPG point selection schemes perform about equally as well as the optimized point selection scheme (scheme C) in the screened charge methods.

Table 4. Averaged Standard Deviation ($\bar{\sigma}_i$) of Charges Derived from the MK, ChElP, and ChElPG Point Selection Schemes Using the Point-Charge Model and the ODS and FDS Models

charge model	PC	ODS[a]	FDS[b]
scaling factor S		1.4	1.6
$(CH_3)_2CO$	0.044	0.028	0.012
$(CH_3)_2SO$	0.174	0.113	0.073
CH_3CN	0.051	0.031	0.038
CH_3OH	0.028	0.005	0.015
ClF	0.014	0.010	0.010
H_2O	0.002	0.002	0.003
H_2S	0.023	0.007	0.018
$H_3SiOHAlH_3$	0.081	0.034	0.033
$H_3SiOSiH_3$	0.072	0.035	0.056
HCl	0.012	0.012	0.012
$HCONH_2$	0.053	0.030	0.011
HF	0.010	0.009	0.008
NH_3	0.012	0.009	0.004
PH_2CHCH_2	0.061	0.027	0.012
PH_3	0.018	0.006	0.004
averaged over 15 molecules	0.044	0.024	0.021

[a]The ODS model with a scaling factor of 1.4. [b]The FDS model with a scaling factor of 1.6.

4.3. Case Study ($HCONH_2$). The formamide molecule, shown in Figure 2, is used as an example to demonstrate the performance of the screened charge models in detail. The effects of the fitting region and ζ values of STOs will be discussed. The PC model and two screened models (i.e., ODS and FDS) are tested. For the two screened charge models, a scaling factor of 1.4 is always used for the ODS model, and 1.6 is used for the FDS model, except in section 4.3.3, where we discuss the effect of the ζ values.

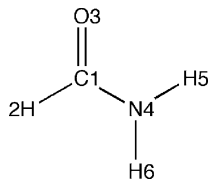

Figure 2. Atom numbering in formamide.

4.3.1. Electrostatic Potential Fitting Using Various Methods. Figure 3 shows the relative root-mean-square error

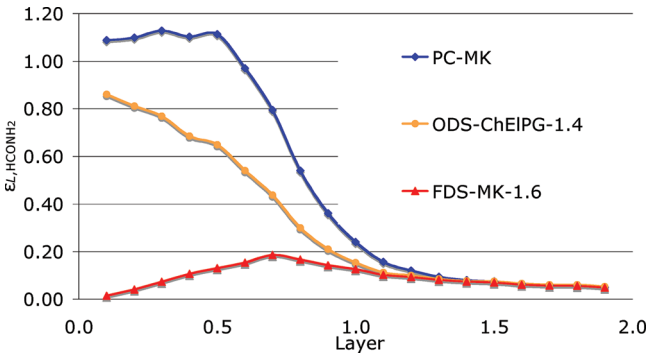

Figure 3. Relative root-mean-square error of electrostatic potentials for each layer using the MK and ChElPG point selection schemes with the point-charge model and the ODS and FDS models. The PC-ChElPG, ODS-MK-1.4, and FDS-ChElPG-1.6 methods (not shown) yield results almost superimposable on the three curves shown.

of electrostatic potentials ($\varepsilon_{L,HCONH2}$) for each layer (see Figure 2) when using the PC model and two screened charge models; $\varepsilon_{L,HCONH2}$ is defined in eq 12. Results from the MK and ChElPG point selection schemes are shown. The PC model fails for the layers that are very close to the nuclei of atoms, and the screened charge methods improve the fitting over all layers. The ODS model improves the fitting in the layers around one van der Waals radius of the centers of atoms, but the error becomes large for the layers that are closer to the centers of atoms. The FDS model improves the fitting over all layers. It is pleasantly surprising that the FDS model can also describe the layers that are very close to the nuclei (even the L = 0.1 layer) very well.

Table 5 shows that there is no significant difference of partial atomic charges derived from the PC model and the screened charge models. In most cases, the advantage of the screened charge models for small molecules is more accurate electrostatic potentials, not more accurate partial atomic charges.

Table 5. Partial Atomic Charges and Dipole Moments of $HCONH_2$ Derived from the Point-Charge Model and the ODS and FDS Models[a]

charge model	PC		ODS		FDS	
point selection scheme	MK	ChElPG	MK	ChElPG[b]	MK[b]	ChElPG
scaling factor S			1.4	1.4	1.6	1.6
C1	0.61	0.67	0.60	0.62	0.59	0.59
H2	0.02	−0.01	0.02	0.01	0.02	0.02
O3	−0.54	−0.56	−0.53	−0.54	−0.53	−0.53
N4	−0.91	−0.89	−0.91	−0.88	−0.91	−0.88
H5	0.43	0.41	0.43	0.41	0.43	0.42
H6	0.39	0.38	0.39	0.38	0.39	0.38
dipole moment (Debye)	3.98	3.99	3.98	3.98	3.99	3.99

[a]The MK and ChElPG point selection schemes are tested. The directly calculated dipole moment is 4.01 D. [b]Recommended methods.

4.3.2. Effect of the Fitting Region. To further test how the fitting region affects the fitting performance of the electrostatic potentials and the fitted charges and dipole moment in the screened charge models, we consider a series of point selection schemes by varying the fitting region (see Table 1). Only the FDS model is tested in this section. Figure 4 shows the relative

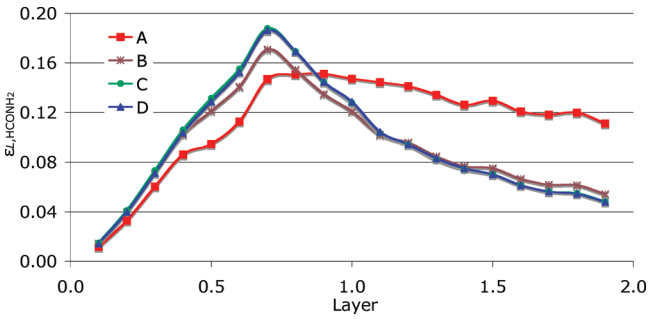

Figure 4. Relative root-mean-square error of electrostatic potentials by the FDS method for each layer using various fitting regions.

root-mean-square error of electrostatic potentials for each layer ($\varepsilon_{L,HCONH2}$) in the four schemes, and Table 6 shows the fitted

Table 6. Partial Atomic Charges and Dipole Moments of $HCONH_2$ Derived from Various Fitting Regions[a]

scheme	A	B	C	D
C1	0.43	0.57	0.58	0.56
H2	0.03	0.02	0.03	0.04
O3	−0.46	−0.52	−0.53	−0.52
N4	−0.68	−0.85	−0.91	−0.89
H5	0.36	0.42	0.43	0.43
H6	0.32	0.37	0.39	0.39
dipole moment	3.75	3.97	4.00	4.00

[a]The directly calculated dipole moment is 4.01 D.

charges and dipole moments in the four schemes. Figure 4 shows that the largest $\varepsilon_{L,HCONH2}$ occurs in layers 0.6, 0.7, and 0.8 in all schemes, possibly because the charge distributions of atoms in the molecule change significantly in the bonding region, and therefore it is harder to describe these regions using the present model. When the fitting points are very close to the atoms, such as in scheme A, the electrostatic potentials of the outer layers cannot be well fitted, and the fitted dipole moments do not agree with the directly calculated ones. When the fitting points are outside one van der Waals radius of the nuclei of any atom, such as in schemes B−D, the fitting performance is good for all layers, and the fitted dipole moments are close to the directly calculated ones. Therefore, only the points outside the van der Waals surface are suitable for electrostatic potential fitting in the screened charge models, and the ChElPG and MK point selection schemes satisfy this criterion.

4.3.3. Effect of the ζ Values of STOs. An important parameter we used in the fitting is the scaling factor S. The scaling factor determines the ζ values of the STOs for all non-H atoms. We tested the fitting performance using various scaling factors. The MK point selection scheme is used for all cases in these figures. Figures 5 and 6 show how the scaling factor affects the relative root-mean-square error of electrostatic potentials ($\varepsilon_{L,HCONH2}$) for each layer in the ODS and FDS models, respectively. Compared with the optimized scaling

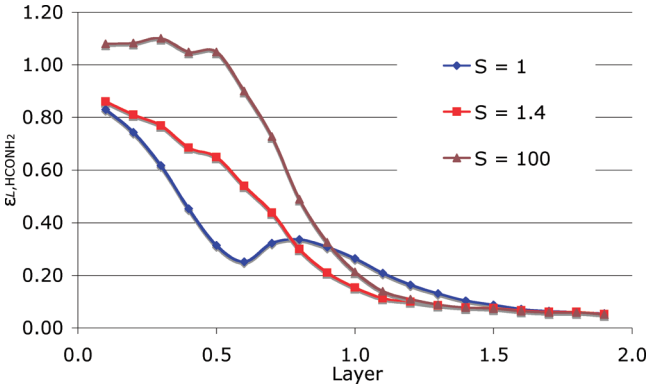

Figure 5. Relative root-mean-square error of electrostatic potentials over each layer using various scaling factors S in the ODS model.

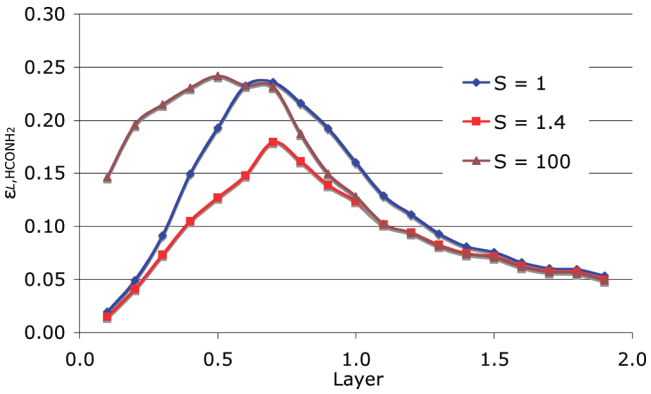

Figure 6. Relative root-mean-square error of electrostatic potentials over each layer using various scaling factors S in the FDS model.

factor, a scaling factor of 100 or 1 gives similar results for the outer layers but much worse results for the inner layers in both the ODS and FDS models. Therefore, a reasonable set of ζ values of STOs in the charge model is necessary for a good fit of electrostatic potentials in all the physical regions. Table 7 shows how the scaling factor affects the fitted charges and dipole moment in the ODS and FDS models. A small scaling factor (i.e., 1) can lead to inaccurate fitted charges and dipole moments, and it is safer to use our recommended scaling factor to derive physical charges.

Table 7. Partial Atomic Charges and Dipole Moments of $HCONH_2$ Derived from the Point-Charge Model and the ODS and FDS Models Using Various Scaling Factors[a]

charge model	PC	ODS		FDS	
scaling factor S		1	100	1	100
C1	0.61	0.51	0.61	0.67	0.59
H2	0.02	0.06	0.02	0.01	0.02
O3	−0.54	−0.50	−0.54	−0.56	−0.53
N4	−0.91	−0.93	−0.91	−0.98	−0.91
H5	0.43	0.45	0.43	0.45	0.43
H6	0.39	0.41	0.39	0.40	0.39
dipole moment (Debye)	3.98	4.04	3.97	3.96	3.99

[a]The MK point selection scheme is used for all cases. The directly calculated dipole moment is 4.01 D.

In the previous study,[29] the ODS model with a scaling factor of 1 for all nonmetal elements showed good performance for the electrostatic interactions. However, since the charge penetration effect is not fully included in the ODS model, the ODS model with a scaling factor of 1 does not fit the electrostatic potentials well. This will be discussed in more detail in section 4.6.

4.4. Restraints on Nonpolar H Atoms. Although in many cases the charges derived from the point-charge model and the screened charge models are similar, we found that in some cases the charges from the point-charge model and screened charge models are different. An example is $(CH_3)_2CO$, shown in Figure 7. Table 8 shows the fitted charges and dipole moments. Comparing the results using the MK and ChElPG point selection schemes, we found that though the fitted charges and dipole moments derived from the screened charge models are more stable than those from the point-charge model, there are some systematic differences between the results from the point-charge model and the screened charge models. In particular, the C−H bonds are more polar in the screened charge models than those in the point-charge model. In previous studies, restraints have been added on certain atoms to get more reliable charges, such as in the RESP method.[13,14] In the present study, we explore the use of restraints on the nonpolar H atoms.

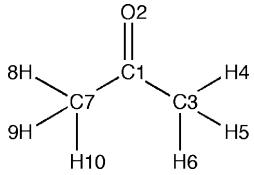

Figure 7. Atom numbering in acetone.

Table 8. Partial Atomic Charges and Dipole Moments of $(CH_3)_2CO$ Derived from the Point-Charge Model and the ODS and FDS Models Using the MK and ChElPG Point Selection Schemes[a]

charge model	PC		ODS		FDS	
point selection scheme	MK	ChElPG	MK	ChElPG	MK	ChElPG
scaling factor S			1.4	1.4	1.6	1.6
C1	0.75	0.70	0.78	0.72	0.80	0.76
O2	−0.54	−0.54	−0.54	−0.53	−0.54	−0.52
C3	−0.55	−0.40	−0.61	−0.53	−0.67	−0.65
H4	0.15	0.10	0.16	0.14	0.18	0.18
H5	0.15	0.10	0.16	0.14	0.18	0.18
H6	0.16	0.12	0.17	0.15	0.19	0.18
C7	−0.56	−0.40	−0.62	−0.53	−0.69	−0.65
H8	0.15	0.10	0.16	0.14	0.18	0.18
H9	0.15	0.10	0.16	0.14	0.18	0.18
H10	0.16	0.12	0.17	0.15	0.19	0.18
dipole moment (Debye)	3.11	3.09	3.10	3.10	3.10	3.11

[a]The directly calculated dipole moment is 3.10 D.

We modified the error function in eq 7 by adding the restraints:

dx.doi.org/10.1021/ct2009285 | J. Chem. Theory Comput. 2012, 8, 1989−1998

Table 9. Charges, Dipole Moments, ε_{all}, and ε_{outer} of $(CH_3)_2CO$ Derived with Various Restraints on Non-Polar H atoms[a]

charge model	PC	ODS				FDS			
λ'	0	0	0.001	0.005	0.01	0	0.001	0.005	0.01
C1	0.75	0.78	0.76	0.70	0.65	0.80	0.78	0.72	0.66
O2	−0.54	−0.54	−0.54	−0.53	−0.52	−0.54	−0.54	−0.53	−0.52
C3	−0.55	−0.61	−0.58	−0.48	−0.39	−0.67	−0.64	−0.52	−0.42
H4	0.15	0.16	0.15	0.13	0.10	0.18	0.17	0.14	0.11
H5	0.15	0.16	0.15	0.13	0.10	0.18	0.17	0.14	0.11
H6	0.16	0.17	0.16	0.14	0.12	0.19	0.18	0.15	0.13
C7	−0.56	−0.62	−0.59	−0.48	−0.39	−0.69	−0.65	−0.53	−0.43
H8	0.15	0.16	0.15	0.13	0.10	0.18	0.17	0.14	0.11
H9	0.15	0.16	0.15	0.13	0.10	0.18	0.17	0.14	0.11
H10	0.16	0.17	0.17	0.14	0.12	0.19	0.18	0.15	0.13
dipole moment (Debye)	3.11	3.10	3.10	3.09	3.08	3.10	3.10	3.09	3.09
ε_{all}	0.47	0.27	0.26	0.26	0.26	0.10	0.10	0.12	0.14
ε_{outer}	0.09	0.06	0.06	0.07	0.08	0.06	0.06	0.07	0.08

[a]The directly calculated dipole moment is 3.10 D.

Table 10. Mean Signed Error (MSE) and Mean Unsigned Error (MUE) of Electrostatic Energies (kcal/mol) Using the QM/MM Method[a]

	equilibrium/acTZ		equilibrium/def2-TZVP		compressed/acTZ		compressed/def2-TZVP		extended/acTZ		extended/def2-TZVP		all	
	MSE	MUE	MSE	MUE	MSE	MUE	MSE	MUE	MSE	MUE	MSE	MUE	MSE	MUE
PC[b]	6.43	6.43	6.43	6.43	14.80	14.80	15.10	15.10	3.02	3.02	2.98	2.98	8.13	8.13
Opt[c]	1.58	1.97	1.32	2.17	3.64	5.09	2.61	5.31	1.06	1.11	1.03	1.16	1.84	2.81
MSB[d]	1.59	2.22	1.19	2.29	3.55	5.39	2.15	5.90	1.07	1.25	1.00	1.24	1.71	3.06
ODS-1.4[e]	4.07	4.08	3.85	4.00	8.15	8.42	7.79	8.33	2.20	2.20	2.15	2.15	4.68	4.86

[a]Accurate values are SAPT electrostatic energies. The first three rows are from Table 6 of ref 29, and the last row shows the results calculated in the present study. [b]Point-charge scheme. [c]ODS with optimized parameters of ref 29. [d]ODS with modified Strand−Bonham (MSB) parameters. [e]ODS with a scaling factor of 1.4.

$$y(q_1, q_2, \ldots q_N) = \sum_{k=1}^{m} [V_k^{QM} - V_k^{ESP}(q_1, q_2, \ldots q_N)]^2 + \lambda' \sum_{\substack{i=1 \\ \text{non-polar H atom}}}^{N_{NPH}} q_i^2 \quad (20)$$

where N_{NPH} is the number of nonpolar H atoms.

We tested the restraints for two well performing schemes, which are the ODS model with a scaling factor of 1.4 and the FDS model with a scaling factor of 1.6, in both cases using the MK point selection scheme. Table 9 shows the fitted charges, dipole moments, and fitting performance with various restraints on nonpolar H atoms. It is found that we can significantly decrease the charges on H atoms compared with the results from the point-charge model while maintaining small $\varepsilon_{all,(CH_3)_2CO}$ and $\varepsilon_{outer,(CH_3)_2CO}$ values. A restraint of $\lambda' = 0.01$ in the ODS and FDS models is suggested for nonpolar H atoms.

4.5. Applications to Charged Molecules and Molecules Containing s-Block and d-Block Elements. The tests described so far are for neutral molecules containing H atoms and p-block elements. To further test the performance of the proposed screened charge schemes, we studied several charged molecules and molecules containing s-block and d-block elements. The geometries and electrostatic potentials are from M06[35,36]/def2-TZVP[41] calculations. The fitted partial atomic charges and fitting performances are shown in the Supporting Information, and the conclusions drawn from these studies are summarized in the rest of this section.

For the three charged molecules, including ClO_3^-, H_3O^+, and NO_3^-, the two screened charge schemes give more stable charges and better fit to the electrostatic potentials than the point-charge model. We conclude that the present method can be applied to the charged species in the same way as it is applied to neutral ones.

For the test of a set of molecules containing s-block and d-block elements, we found that the performance is not as good as for the H atom and p-block elements; however, the method still appears useful. In addition to the FDS method, the tables show the results for the ODS method and also for a method denoted as "ODS (H and p-block)" in the tables—the last named option corresponds to the ODS scheme with only the H atom and p-block atoms being screened. For 14 test cases, with both MK and ChElPG point selection, that makes a total of 84 possible comparisons to the point charge method, and in all 84 cases, we find that ε_{all} is improved. However, when one looks only at ε_{outer}, we find that FDS improves the results only about half the time. ODS improves them most of the time, and ODS (H and p-block) always improves them or at least does as well as point charges. Therefore, on average, for molecules containing s-block and d-block elements, the ODS model works better than the FDS model and the point-charge model. We think that for s-block and d-block elements, the charge penetration effects are more difficult to take into account, and certainly the present models oversimplify the problem. The present models should be used with caution for systems containing s and d block elements, although the ODS (H and p-block) scheme seems safe, and FDS appears safe when the s-

Table 11. MSE and MUE of the Induction Energies (kcal/mol) Using the QM/MM Method[a]

	equilibrium/acTZ		equilibrium/def2-TZVP		compressed/acTZ		compressed/def2-TZVP		extended/acTZ		extended/def2-TZVP		all	
	MSE	MUE	MSE	MUE	MSE	MUE	MSE	MUE	MSE	MUE	MSE	MUE	MSE	MUE
PC[b]	0.67	1.09	1.12	1.18	3.46	3.98	4.34	4.46	0.12	0.45	0.35	0.38	1.72	1.94
Opt[c]	−0.74	1.00	0.69	0.82	−0.62	2.67	2.68	3.13	−0.34	0.45	0.25	0.30	0.46	1.40
MSB[d]	−0.79	1.02	0.68	0.80	−0.71	2.65	2.60	3.12	−0.36	0.46	0.25	0.29	0.42	1.39
ODS-1.4[e]	−0.28	1.01	0.75	0.82	0.77	2.56	3.14	3.31	−0.20	0.48	0.24	0.28	0.84	1.42

[a]Accurate values are SAPT damped induction energies. The first three rows are from Table 7 of ref 29, and the last row shows the results calculated in the present study. [b]Point-charge scheme. [c]ODS with optimized parameters of ref 29. [d]ODS with modified Strand−Bonham (MSB) parameters. [e]ODS with a scaling factor of 1.4.

block and d-block elements are surrounded by H and p-block elements.

4.6. Limitations and Improvements and Comments on Combined QM/MM Calculations. Although the two screened charge models improve the fitting performance of the electrostatic potentials, both models have disadvantages.

In the ODS model, the charge density of an atom is assumed to be the sum of a point-charge and a smeared charge. This model has been shown to be a good compromise for calculating the QM/MM electrostatic energy and avoiding overpolarization in the QM/MM method.[29] However, this model only includes part of the charge penetration effect since only n_{screen} electrons are in the screening distribution. Since the previous ζ values of STOs were parametrized to best reproduce the directly calculated electrostatic and induction energies,[29] these parameters compensate for the approximation of the ODS model. Therefore, the same set of parameters does not reproduce the electrostatic potentials as well as the new parameters optimized for that purpose in the present work, as shown in section 4.3.3. To test how well the new set of parameters works for the QM/MM electrostatic and induction energies, we carried out the same QM/MM calculations as presented in ref 29 but now with the new parameters. The comparison is shown in Tables 10 and 11. As in ref 29, we separate the tests into equilibrium geometries, compressed geometries (the severest test), and expanded geometries, and we show two results for two different basis sets for the QM region: acTZ, which is short for aug-cc-pVTZ,[42,43] and def2-TZVP.[41] The last column is averaged over the previous 12 columns and provides a summary. The first three rows of these two tables are from Tables 6 and 7 of ref 29, and the last rows of these two tables show the results with the new parameters (i.e., 1.32 for the H atom and a scaling factor of 1.4 for non-H atoms). The new set of parameters performs worse than the optimized parameters for the QM/MM electrostatic energy and induction energy but still greatly improves the results compared with the point-charge method. Therefore, the ODS model with the new set of parameters can be used to calculate both the QM/MM electrostatic and induction energies and the electrostatic potentials, while the previous set of parameters in ref 29 should only be used to calculate the QM/MM electrostatic and induction energies.

In the FDS model, the delocalization character of the electrons is well described, even for the regions that are close to the nuclei of atoms in a molecule. The fitted charges can be useful to calculate the electrostatic energies in MM calculations. However, the FDS screened charge model may not be useful for QM/MM calculations if no Pauli exchange is added in SCF calculations because it greatly overestimates the magnitudes of induction energies when one includes induction without exchange repulsion. This is more of a comment on the incompleteness of the combined QM/MM method, as usually implemented, than a limitation of the FDS screened electrostatic model.

Another issue to be considered with regard to the FDS model is that the charge density of the neutral atom may not be a good reference density for highly charged atoms. The charge density of a highly charged atom can be significantly different from that of the neutral atom, and the current model may not be appropriate. One way to overcome this drawback of the FDS model is to take the effective charge as the linear combination of the neutral atom and the charged atoms, with the weighting factor determined by the charge q_A. The effective charge of atom A is expressed as

$$q_A^*(r) = \theta(-q_A)[(-q_A)\, Z_{eff}^{anion}(r) + (1 + q_A)\, Z_{eff}^{neutral}(r)] + \theta(q_A)[(q_A) Z_{eff}^{cation}(r) + (1 - q_A) Z_{eff}^{neutral}(r)] \quad (21)$$

where $Z_{eff}^{anion}(r)$, $Z_{eff}^{neutral}(r)$, and $Z_{eff}^{cation}(r)$ are the effective charges of the atom in its anion, neutral, and cation forms, and $\theta(x)$ denotes a Heaviside function of x.

5. CONCLUSIONS

In the present study, we propose a new kind of screened charge model to derive partial atomic charges using ESP fitting, and we compare its performance to the conventional point-charge model and to a previous screened charge method. In the screened charge models, the charges are more stable with respect to the point selection schemes, and the fitting performance is better than with the point-charge model.

The ODS model with a scaling factor (S) of 1.4 and the FDS model with a scaling factor of 1.6, combined with either the ChElPG or MK point selection scheme, have shown good fitting performance and are recommended for use. In particular, our final recommended method for electrostatic potentials is FDS-MK-1.6. However, the scheme should be used carefully if there are s-block and d-block elements in the molecules. In those cases, ODS-MK-1.4 gives better performance based on our experience. Our recommended method for combined QM/MM calculations is ODS-ChElPG-S with $1.0 \leq S \leq 1.4$.

■ ASSOCIATED CONTENT

Supporting Information

The fitted charges and fitting performance of the molecules tested in section 4.5. This information is available free of charge via the Internet at http://pubs.acs.org.

AUTHOR INFORMATION

Corresponding Author

*E-mail: truhlar@umn.edu.

Notes

The authors declare no competing financial interest.

ACKNOWLEDGMENTS

This work was supported by the National Science Foundation under grant no. CHE09-56776.

REFERENCES

(1) Storer, J. W.; Giesen, D. J.; Cramer, C. J.; Truhlar, D. G. *J. Comput.-Aided Mol. Des.* **1995**, *9*, 87−110.
(2) Rappe, A. K.; Goddard, W. A. *J. Phys. Chem.* **1991**, *95*, 3358−3363.
(3) Mulliken, R. *J. Chem. Phys.* **1955**, *23*, 1833−1840.
(4) Baker, J. *Theor. Chem. Acc.* **1985**, *68*, 221−229.
(5) Hirshfeld, F. L. *Theor. Chim. Acta* **1977**, *44*, 129−138.
(6) Bultinck, P.; Van Alsenoy, C.; Ayers, P. W.; Carbo-Dorca, R. *J. Chem. Phys.* **2007**, *126*, 144111.
(7) Lillestolen, T. C.; Wheatley, R. J. *Chem. Commun.* **2008**, 5909−5911.
(8) Momany, F. A. *J. Phys. Chem.* **1978**, *82*, 592−601.
(9) Cox, S. R.; Williams, D. E. *J. Comput. Chem.* **1981**, *2*, 304−323.
(10) Singh, U. C.; Kollman, P. A. *J. Comput. Chem.* **1984**, *5*, 129−145.
(11) Chirlian, L. E.; Francl, M. M. *J. Comput. Chem.* **1987**, *8*, 894−905.
(12) Breneman, C. M.; Wiberg, K. B. *J. Comput. Chem.* **1990**, *11*, 361−373.
(13) Bayly, C. I.; Cieplak, P.; Cornell, W. D.; Kollman, P. A. *J. Phys. Chem.* **1993**, *97*, 10269−10280.
(14) Laio, A.; VandeVondele, J.; Rothlisberger, U. *J. Phys. Chem. B* **2002**, *106*, 7300−7307.
(15) Hu, H.; Lu, Z. Y.; Yang, W. *J. Chem. Theory Comput.* **2007**, *3*, 1004−1013.
(16) Chen, D. L.; Stern, A. C.; Space, B.; Johnson, J. K. *J. Phys. Chem. A* **2010**, *114*, 10225−10233.
(17) Kelly, C. P.; Cramer, C. J.; Truhlar, D. G. *Theor. Chem. Acc.* **2005**, *113*, 133−151.
(18) Kelly, C. P.; Cramer, C. J.; Truhlar, D. G. *J. Chem. Theory Comput.* **2005**, *1*, 1133−1152.
(19) Olson, R. M.; Marenich, A. V.; Cramer, C. J.; Truhlar, D. G. *J. Chem. Theory Comput.* **2007**, *3*, 2046−2054.
(20) Francl, M. M.; Carey, C.; Chirlian, L. E.; Gange, D. M. *J. Comput. Chem.* **1996**, *17*, 367−383.
(21) Day, P. N.; Jensen, J. H.; Gordon, M. S.; Webb, S. P.; Stevens, W. J.; Krauss, M.; Garmer, D.; Basch, H.; Cohen, D. *J. Chem. Phys.* **1996**, *105*, 1968−1986.
(22) Freitag, M. A.; Gordon, M. S.; Jensen, J. H.; Stevens, W. J. *J. Chem. Phys.* **2000**, *112*, 7300−7306.
(23) Piquemal, J. P.; Gresh, N.; Giessner-Prettre, C. *J. Phys. Chem. A* **2003**, *107*, 10353−10359.
(24) Cisneros, G. A.; Piquemal, J. P.; Darden, T. A. *J. Phys. Chem. B* **2006**, *110*, 13682−13684.
(25) Piquemal, J. P.; Cisneros, G. A.; Reinhardt, P.; Gresh, N.; Darden, T. A. *J. Chem. Phys.* **2006**, *124*, 104101.
(26) Werneck, A. S.; Filho, T. M. R.; Dardenne, L. E. *J. Phys. Chem. A* **2007**, *112*, 268−280.
(27) Cisneros, G. A.; Tholander, S. N.-I.; Parisel, O.; Darden, T. A.; Elking, D.; Perera, L.; Piquemal, J. P. *Int. J. Quantum Chem.* **2008**, *108*, 1905−1912.
(28) Elking, D. M.; Cisneros, G. A.; Piquemal, J. P.; Darden, T. A.; Pedersen, L. G. *J. Chem. Theory Comput.* **2010**, *6*, 190−202.
(29) Wang, B.; Truhlar, D. G. *J. Chem. Theory Comput.* **2010**, *6*, 3330−3342.
(30) Stone, A. J. *J. Phys. Chem. A* **2011**, *115*, 7017−7027.
(31) Tafipolsky, M.; Engels, B. *J. Chem. Theory Comput.* **2011**, *7*, 1791−1803.
(32) Strand, T. G.; Bonham, R. A. *J. Chem. Phys.* **1964**, *40*, 1686−1691.
(33) Mantina, M.; Valero, R.; Cramer, C. J.; Truhlar, D. G. Atomic Radii of the Elements. In *CRC Handbook of Chemistry and Physics*, 92nd ed.; Haynes, W. M., Ed.; CRC Press: Boca Raton, FL, 2011−2012; pp 9−49f.
(34) Frisch, M. J.; Trucks, G. W.; Schlegel, H. B.; Scuseria, G. E.; Robb, M. A.; Cheeseman, J. R.; Montgomery, J. A., Jr.; Vreven, T.; Kudin, K. N.; Burant, J. C.; Millam, J. M.; Iyengar, S. S.; Tomasi, J.; Barone, V.; Mennucci, B.; Cossi, M.; Scalmani, G.; Rega, N.; Petersson, G. A.; Nakatsuji, H.; Hada, M.; Ehara, M.; Toyota, K.; Fukuda, R.; Hasegawa, J.; Ishida, M.; Nakajima, T.; Honda, Y.; Kitao, O.; Nakai, H.; Klene, M.; Li, X.; Knox, J. E.; Hratchian, H. P.; Cross, J. B.; Bakken, V.; Adamo, C.; Jaramillo, J.; Gomperts, R.; Stratmann, R. E.; Yazyev, O.; Austin, A. J.; Cammi, R.; Pomelli, C.; Ochterski, J. W.; Ayala, P. Y.; Morokuma, K.; Voth, G. A.; Salvador, P.; Dannenberg, J. J.; Zakrzewski, V. G.; Dapprich, S.; Daniels, A. D.; Strain, M. C.; Farkas, O.; Malick, D. K.; Rabuck, A. D.; Raghavachari, K.; Foresman, J. B.; Ortiz, J. V.; Cui, Q.; Baboul, A. G.; Clifford, S.; Cioslowski, J.; Stefanov, B. B.; Liu, G.; Liashenko, A.; Piskorz, P.; Komaromi, I.; Martin, R. L.; Fox, D. J.; Keith, T.; Al-Laham, M. A.; Peng, C. Y.; Nanayakkara, A.; Challacombe, M.; Gill, P. M. W.; Johnson, B.; Chen, W.; Wong, M. W.; Gonzalez, C.; Pople, J. A. *Gaussian 09*, version A. 02; Gaussian, Inc.: Wallingford, CT, 2009.
(35) Zhao, Y.; Truhlar, D. G. *Acc. Chem. Res.* **2008**, *41*, 157−167.
(36) Zhao, Y.; Truhlar, D. G. *Theor. Chem. Acc.* **2008**, *120*, 215−241.
(37) Hehre, W. J.; Ditchfield, R.; Pople, J. A. *J. Chem. Phys.* **1972**, *56*, 2257−2261.
(38) Dill, J. D.; Pople, J. A. *J. Chem. Phys.* **1975**, *62*, 2921−2923.
(39) Francl, M. M.; Pietro, W. J.; Hehre, W. J.; Binkley, J. S.; Gordon, M. S.; DeFrees, D. J.; Pople, J. A. *J. Chem. Phys.* **1982**, *77*, 3654−3665.
(40) Lynch, B. J.; Zhao, Y.; Truhlar, D. G. *J. Phys. Chem. A* **2003**, *107*, 1384−1388.
(41) Weigend, F.; Ahlrichs, R. *Phys. Chem. Chem. Phys.* **2005**, *7*, 3297−3305.
(42) Dunning, T. H., Jr. *J. Chem. Phys.* **1989**, *90*, 1007−1023.
(43) Kendall, R. A.; Dunning, T. H., Jr.; Harrison, R. J. *J. Chem. Phys.* **1992**, *96*, 6796−6806.